

## Traffic flow on pedestrianized streets

Daganzo, CF; Knoop, VL

**DOI**

[10.1016/j.trb.2015.12.017](https://doi.org/10.1016/j.trb.2015.12.017)

**Publication date**

2016

**Document Version**

Final published version

**Published in**

Transportation Research. Part B: Methodological

**Citation (APA)**

Daganzo, CF., & Knoop, VL. (2016). Traffic flow on pedestrianized streets. *Transportation Research. Part B: Methodological*, 86(April), 211-222. <https://doi.org/10.1016/j.trb.2015.12.017>

**Important note**

To cite this publication, please use the final published version (if applicable).  
Please check the document version above.

**Copyright**

Other than for strictly personal use, it is not permitted to download, forward or distribute the text or part of it, without the consent of the author(s) and/or copyright holder(s), unless the work is under an open content license such as Creative Commons.

**Takedown policy**

Please contact us and provide details if you believe this document breaches copyrights.  
We will remove access to the work immediately and investigate your claim.

***Green Open Access added to TU Delft Institutional Repository***

***'You share, we take care!' - Taverne project***

**<https://www.openaccess.nl/en/you-share-we-take-care>**

Otherwise as indicated in the copyright section: the publisher is the copyright holder of this work and the author uses the Dutch legislation to make this work public.



# Traffic flow on pedestrianized streets



Carlos F. Daganzo<sup>a,\*</sup>, Victor L. Knoop<sup>b</sup>

<sup>a</sup> Department of Civil and Environmental Engineering, 416 McLaughlin Hall #1720, The University of California, Berkeley, Berkeley, CA 94720, United States

<sup>b</sup> Transport & Planning Department, Delft University of Technology, Stevinweg 1, 2628 CN Delft, The Netherlands

## ARTICLE INFO

### Article history:

Received 3 August 2015

Revised 30 December 2015

Accepted 31 December 2015

### Keywords:

Traffic flow

Pedestrians

Queuing theory

MFD

## ABSTRACT

Giving pedestrians priority to cross a street enhances pedestrian life, especially if crosswalks are closely spaced. Explored here is the effect of this management decision on car traffic. Since queuing theory suggests that for a given pedestrian flux the closer the crosswalk spacing the lower the effect of pedestrians on cars, scenarios where pedestrians can cross anywhere should be best for both cars and pedestrians. This is the kind of pedestrianization studied.

Analytic formulas are proposed for a pedestrianized street's capacity, free-flow speed and macroscopic fundamental diagram. Of these, only the free-flow speed formula is exact. The analytic form of the capacity formula is inspired by analytic upper and lower bounds derived with variational theory for a version of the problem where cars are treated as a fluid. The formula is then calibrated against microscopic simulations with discrete cars. The MFD for the fluid version of the problem is shown to be concave and have a certain symmetry. These two geometrical properties, together with the formulae for capacity and free-flow speed, yield a simple approximation for the MFD.

Both the capacity and MFD formulae match simulations with discrete cars well for all values of the pedestrian flux – errors for the capacity are well under 0.2% of the capacity before pedestrianization. Qualitatively, the formulas predict that the street's capacity is inversely proportional to the square root of the pedestrian flux for low pedestrian fluxes, and that pedestrians increase the cars' free-flow pace by an amount that is proportional to the pedestrian flux.

© 2016 Elsevier Ltd. All rights reserved.

## 1. Introduction to the problem

In urban environments, traffic flow is affected by the external influence of pedestrians. If pedestrians are regulated by traffic lights the only disruptions to flow are the traffic light themselves. This situation is simple and formulas to predict delay already exist; see e.g. Daganzo (1977). Therefore this paper focuses on the unsignalized case. The subcase in which cars have priority over pedestrians is not interesting because (i) pedestrians have no effect on traffic flow and (ii) the ensuing pedestrian delays have already been described with queuing theory (Tanner, 1951). Therefore the focus is narrowed to the subcase in which pedestrians have priority at all crossings.

We want to understand the effect of these crossings on the traffic stream. The effect of a single crosswalk is already well understood. Queuing formulas, in which the cars are customers served by the crosswalk, exist for both the street capacity

\* Corresponding author. Tel.: +1 510 642 3853.

E-mail address: [daganzo@ce.berkeley.edu](mailto:daganzo@ce.berkeley.edu) (C.F. Daganzo).

and the expected traffic delay (Daganzo, 1997; Hawkes, 1965; 1968). These formulas predict that splitting the pedestrian flow of a single crosswalk among several widely separated crosswalks always increases the street's capacity and reduces car delay; i.e., that a street design with crosswalks, say, every 25 m is better for cars than one with crosswalks every 100 m. We conjecture that this continues to be true if the crosswalk separation tends to zero; i.e., if we allow pedestrians to cross anywhere. Since crossing anywhere is also good for pedestrians, it is probably the best thing to do if pedestrians are to have priority. This pedestrianization shall be the scenario considered in this paper.

A street with multiple pedestrian crosswalks can be modeled as a serial queuing system. However, when the crosswalks are very closely spaced, car queues will spill back over upstream crosswalks, “blocking” service. Unfortunately, queuing theory does not provide easy answers to problems with spillbacks – the solution with only two servers is already very complicated; see Newell (1979). For this reason, our crossing-anywhere scenario will not be studied here with the tools of queuing theory, but with a combination of symmetry arguments, dimensional analysis, simulation and traffic flow theory.

We shall consider an infinitely long homogeneous street with cars and crossing pedestrians. It is assumed that cars behave according to the kinematic wave theory (KWT) of traffic flow (Lighthill and Whitham, 1955; Richards, 1956), and that the fundamental diagram relating flow  $q$ , and density  $k$ , is triangular as proposed in Newell (1993). The fundamental diagram (FD) relationship is denoted  $q = Q(k)$ . As is well known, kinematic wave theory is equivalent to two other representations of traffic that will be used in this paper: (i) the variational theory (VT) of traffic flow with a linear cost function (Daganzo, 2005; 2005a; 2006); and (ii) Newell's simplified car-following model (Newell, 2002). Pedestrian arrivals are assumed to be homogeneous in space, stationary in time and mutually independent. Each pedestrian is assumed to interrupt traffic for a fixed amount of time, which is equal for all pedestrians. We are interested in seeing how these random interruptions modify the macroscopic fundamental diagram (MFD) of the street, and in particular how much they reduce the street's capacity and its free-flow speed.

To answer these questions the paper is organized as follows. Section 2 formulates the problem in the continuum world of KWT/VT in which cars are treated like a fluid, and then shows that a one-parameter family of curves depicts the MFDs for all scenarios. Section 3 derives an expression for the maxima of these curves, i.e., the pedestrianized street's capacity, and compares it with discrete car-following simulations. Section 4 then presents an exact formula for the free-flow speed and an approximate analytic formula for the MFD that is also compared with simulations. Finally, Section 5 presents some conclusions

## 2. Formulation

This section formulates the problem in a continuum framework where cars are treated like a fluid. After some simplifications, described in Section 2.1, the problem is stated in the context of variational theory.

### 2.1. Simplifications

The MFD of a generic pedestrianized street is sought. To define an instance of the problem one needs to characterize the street and the pedestrians. Since the street has a triangular FD, three parameters suffice to describe it. We shall use: (i) the street capacity without pedestrians,  $q_0$ ; (ii) the jam density  $k_j$ ; and (iii) the optimum density,  $k_o$ . Other FD features can be derived from these three parameters. This paper will use: (a) the free-flow speed,  $v_f = q_0/k_o$ ; (b) the backward wave speed,  $w = q_0/(k_j - k_o)$ ; and (c) the flow-intercept of the congested branch,  $r = k_j q_0/(k_j - k_o)$ .

To describe the pedestrians two parameters suffice. We shall use: (iv) their arrival flux  $f$  in pedestrians per unit time per unit length of street; and (v) the time,  $\tau$ , that each pedestrian blocks the street. Thus, an instance of the problem is defined by five parameters in total.

To simplify the formulation we shall choose the units for time, distance and vehicle number ( $u_t, u_x, u_n$ ) such that the values of  $\tau$ ,  $q_0$  and  $k_j$  equal 1. The reader can verify that this is always possible by choosing ( $u_t \equiv \tau$ ,  $u_n \equiv q_0 \tau$ ,  $u_x \equiv q_0 \tau / k_j$ ). For example, if  $q_0 = 1800$  v/h,  $k_j = 200$  v/km and  $\tau = 5$  s then  $u_t = 5$  s,  $u_n = 2.5$  v and  $u_x = 12.5$  m. Thus, from now on and without any loss of generality:  $\tau = q_0 = k_j = 1$  so that these parameters are eliminated.

In order to eliminate one additional parameter from the problem (the value of  $k_o$ ), we shall work in a system of asynchronous time-space coordinates such the the clock is started at every location,  $x$ , with the passage of an observer moving at speed  $u$ ; i.e., so that in our chosen coordinate system time is defined by:

$$t' = t - x/u. \quad (1)$$

As explained in Daganzo (2002), this transformation preserves the KW character of the traffic problem regardless of the chosen  $u$ . (The special case with  $u = v_f$  was previously used in Newell, 1993). The reader can verify that (1) leaves invariant the flow but changes the speed and density variables as follows:

$$1/v' = 1/v - 1/u, \quad (2)$$

and

$$k' = k - Q(k)/u. \quad (3)$$

To eliminate  $k_o$  choose any desired constant,  $c \in [0, 1]$ , and let the observer pace be  $1/u = k_o - c$ . Then, as shown by (3), the optimum density becomes  $k'_o = k_o - Q(k_o)(k_o - c) = k_o - (k_o - c) = c$ . The value  $c = 1/2$  is adopted in this paper as it

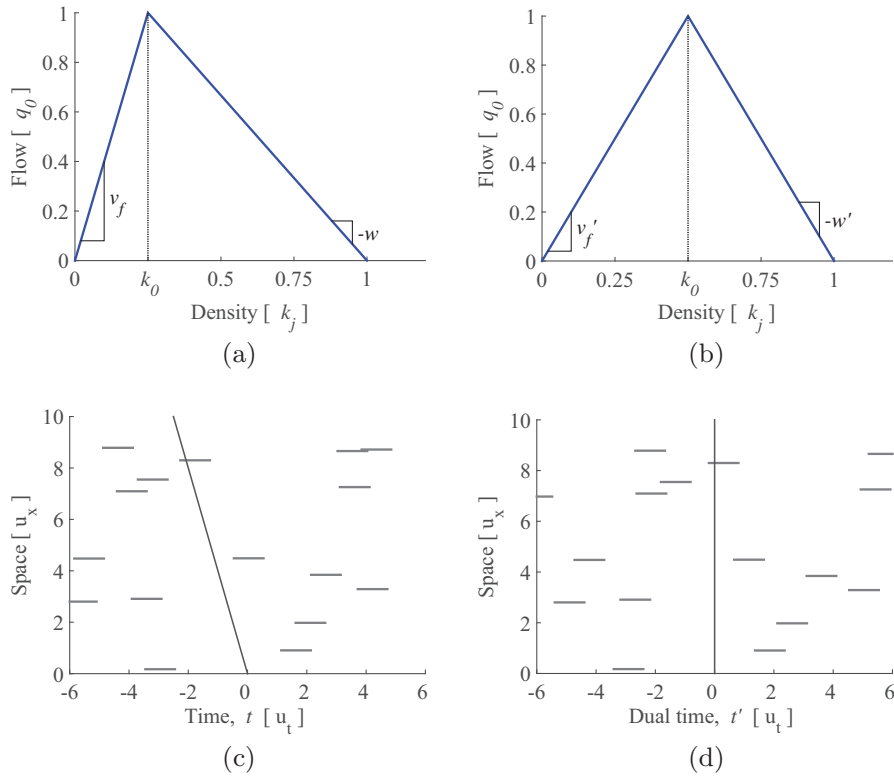


**Fig. 1.** The primal-dual transformation [symbols in brackets are the measurement units]: (a) a primal FD; (b) the symmetric dual FD; (c) a primal pedestrian realization with the observer's trajectory; (d) dual image of the primal realization and the transformed observer trajectory.

yields a symmetric FD; see Fig. 1a and b. Curiously, Laval and Castrillon (2015) have recently rediscovered the asynchronous time transformation in the context of a different problem, and also chose to work with a symmetric MFD.

This symmetry is in agreement with (2), which indicates that the free-flow and backward wave speeds become equal and of opposite sign – since  $1/v'_f = 1/v_f - (k_0 - 1/2) = k_0 - k_0 + 1/2 = 1/2$  and  $1/(-w') = 1/(-w) - (k_0 - 1/2) = (k_0 - 1) - k_0 + 1/2 = -1/2$ . Thus, the chosen transformation converts a street with arbitrary  $k_0$  into one with symmetric limiting speeds,  $v'_f = w' = 2$ , and  $k'_0 = 1/2$  as shown in Fig. 1b. We shall call the problem and the FD as originally formulated “primal”, and the ones arising from the change of variable “dual”.

The primal-dual transformation would be useless if it changed the character of the pedestrians, but this is not the case. Note that our bottlenecks have infinite pace, which is preserved by (2).<sup>1</sup> Also note that (1) converts any set of points in the primal time-space plane  $(t, x)$  into a unique image in the dual plane,  $(t', x)$ , and viceversa – i.e., the transformation is a bijection. In particular, the transformation associates with every (primal) draw of a pedestrian realization a unique dual image, as illustrated by Fig. 1c and d. Furthermore, since the transformation is linear, it preserves for these dual images the defining properties of primal pedestrian arrivals; i.e., their homogeneous, stationary and independent nature; and their arrival flux,  $f \geq 0$ . Thus, the dual images of the random primal realizations can be interpreted themselves as random realizations of a dual problem of the same type as the original, albeit with a transformed FD.

In summary, the only difference between the primal and the dual problems is that the optimum density of the dual is  $k'_0 = 1/2$  instead of  $k_0$ . From now on and without any loss of generality we shall work in the dual plane, so the primes will be dropped. In this plane, the optimum density is fixed so that the only free parameter that can influence the MFD is  $f$ . In other words, the set of (dual) MFDs for all problems is a one-parameter family of curves,  $Q(k|f)$ . This family will be the focus of this paper. (Boldface shall be used from now on for variables and functions representing pedestrianized conditions.)

The parameter  $f$  can be interpreted as the expected number of pedestrian arrivals to a section of street of length  $u_x$  (comparable with a few car spacings) during a time  $\tau$  (consisting of a few seconds). In most real applications arrivals in such a narrow window should be rare so that typically  $f \ll 1$ . For larger  $f$  pre-timed pedestrian traffic lights are a better option since their effect on both cars and pedestrians is largely independent of  $f$ .

<sup>1</sup> A seemingly similar problem – moving bottlenecks due to lane changes in weaving areas – cannot be simplified in the same manner because in this case (2) changes the bottlenecks' speeds.

## 2.2. The modeling framework

To start, let us define two technical terms: (i) “pedestrian realization”, or “realization” for short: a randomly drawn set of pedestrian arrival points in the time-space plane,  $\{\dots, (t_i, x_i), \dots\}$ ; and (ii) “conditional capacity”: the street’s maximum flow possible for a given pedestrian realization. The street’s capacity, denoted  $q_o$ , is the average of the conditional capacities across an infinite number of pedestrian realizations. Section 3 below is devoted to finding the function  $q_o(f)$ .

The pedestrian interruptions of a given realization shall be modeled as fixed bottlenecks with zero capacity, each pinned at  $x_i$  and lasting from  $t_i$  to  $t_i + 1$ . Variational theory will be used to evaluate the street’s conditional capacity given the bottlenecks. The following definitions and general facts from VT pertaining to problems with triangular FDs will be used – see Daganzo (2005a; 2005b) for justifications:

- Definition 1: A path is “valid” if the slope between any two of its points is in  $[-w, v_f]$ .
- Definition 2: Slopes equal to  $v_f$  or  $-w$  are called “extremal”.
- Definition 3: A path is “feasible” if it is, both, valid, and goes from the origin to a point  $(T, 0)$  on the time axis. The time  $T$  is the path’s “duration”.
- Fact 1: The conditional capacity is the least cost of all feasible paths with  $T \rightarrow \infty$ .
- Fact 2: The cost per unit time of a path segment with extremal slope  $v_f$  is 0.
- Fact 3: The cost per unit time of a path segment with slope 0 (not on a bottleneck) is  $q_o$ .
- Fact 4: The cost per unit time of a path segment with extremal slope  $-w$  is the flow-intercept of the FD’s congested branch,  $r \equiv 1/(1 - k_o)$ .
- Fact 5: If a path segment is entirely on a bottleneck its cost rate is 0.
- Fact 6: Without bottlenecks, all valid paths joining two points have the same cost.

With these preliminaries out of the way, the analysis now begins.

## 3. The street capacity

The function  $q_o(f)$  is now characterized. Analytic bounds based on VT are derived in Sections 3.1 and 3.2. Building on these bounds, an approximation is then proposed in Section 3.3. The approximation is calibrated and verified with discrete car-following simulations.

### 3.1. An upper bound

An upper bound is given by the expected cost of any feasible path. Therefore, an algorithm that yields reasonably cheap piecewise linear paths and allows the expected cost to be expressed analytically is sought.

Since all our bottlenecks have zero speed, the cost of a feasible path is the amount of time when it does not overlap with bottlenecks.<sup>2</sup> Thus, the proposed algorithm shall look for paths with low non-overlap times. To facilitate analysis, the algorithm is myopic, considering one pedestrian bottleneck at a time and adding a path portion that includes said bottleneck. To make the bound as tight as possible, the greediest selection criterion in terms of cost is used. This criterion is the ratio of non-overlap to overlap durations of the portion added. This ratio will be called from now on the “n-ratio”.

Each step of the algorithm produces two consecutive linear segments. The first reaches a pedestrian bottleneck and the second follows it. In order to minimize the n-ratio for each added bottleneck, bottlenecks are always reached at the earliest time possible and then followed for their remaining durations.

The pedestrian is chosen with two objectives in mind: (i) minimizing the “n-ratio”; and (ii) ensuring that the path returns to the horizontal axis with probability 1, so it is feasible for  $T \rightarrow \infty$ .

Fig. 2 illustrates the pedestrian selection procedure. The origin in that figure is at the end point of the previous step. The pedestrian is chosen with the help of a family of isosceles triangles such as ACD in the figure, with a common vertex A at point  $(-1, 0)$ , and two other vertices C and D. The latter are located where the two rays emanating from the origin with extremal slopes  $(-2$  and  $2)$  reach ordinates  $+z$  and  $-z$ . Note that the time separation between a triangle’s vertical side CD and the vertical axis is  $z/2$ . To select the pedestrian, first identify the triangle with the smallest  $z$  that includes a pedestrian arrival and then choose any of these pedestrians. Note this pedestrian must arrive on the triangle’s border.

The significance of the family is that the triangles’ borders are the loci of all possible pedestrian arrivals with n-ratio,  $z/2$ .<sup>3</sup> Thus, our selection method minimizes the n-ratio in agreement with objective (ii). Furthermore, because the procedure has mirror symmetry with the horizontal axis, its steps produce a null-recurrent random walk that is sure to return to the horizontal axis as the number of steps tends to infinity – see e.g., Feller (1968). Thus, objective (i) is also satisfied.

<sup>2</sup> Let the path be of duration  $T$  and overlap with bottlenecks for duration  $O$ . If the bottlenecks are not active the path’s cost is  $T$  (by virtue of Facts 3 and 4) and the cost of the overlapping portion is  $O$  (by virtue of Fact 3). If the bottlenecks are activated the latter cost is reduced to zero (by virtue of Fact 5). Thus the cost after activation is  $T - O$ ; i.e., the amount of time the path does not overlap with bottlenecks.

<sup>3</sup> Note how all arrivals on side CD exhibit non-overlap duration  $z/2$ , and overlap duration, 1; thus their n-ratio is  $z/2$ . Arrivals on sides AC or AD, say with ordinate  $x$ , can be reached with an extremal ray in time  $|x|/2$ , and this occurs when the bottleneck has already lasted for  $1 - |x|/z$  time units. Thus, the overlap duration is  $|x|/z$  and the n-ratio is  $(|x|/2)/(|x|/z) = z/2$ .

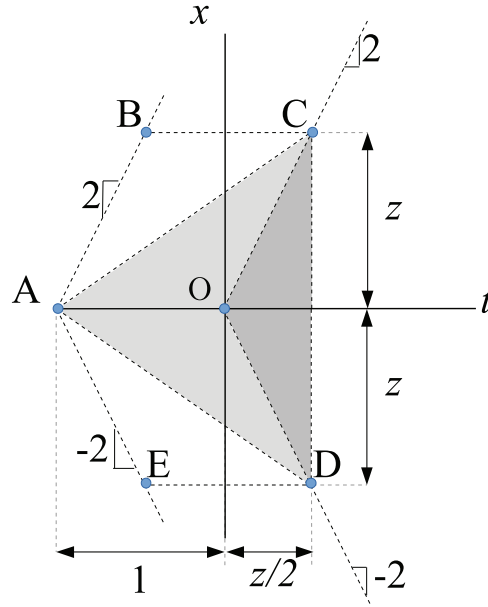


Fig. 2. Geometrical regions used to construct the capacity bounds.

Now, designate by  $L_i$  the duration of the  $i$ th non-overlapping segment and by  $O_i$  the duration of the following overlapping segment. Then the path's conditional upper bound (i.e. the ratio of the path's cost with and without bottlenecks) is:  $\sum L_i / (\sum O_i + \sum L_i)$ . Since our problem is homogeneous in time-space, the terms in each of these summations are identically distributed. Thus, as the number of pedestrians tends to infinity the summations can be replaced by expectations so that:  $\sum L_i / (\sum O_i + \sum L_i) = E(L) / (E(L) + E(O))$ . This shows that the conditional upper bound is the same for all realizations. Hence,  $q_o^U = E(L) / (E(L) + E(O))$ . Expressions for  $E(L)$  and  $E(O)$  are now derived.

Let us first derive the expectations  $E(L|z)$  and  $E(O|z)$ , conditional on the  $z$ -value of the chosen pedestrian. To this end, consider the lighter and darker shaded regions of Fig. 2. The quadrilateral ACOD, of size  $A_1(z) = z$ , is the locus of pedestrian arrival points with  $n$ -ratio smaller than  $z/2$  and partial overlap. The triangle OCD, of size  $A_2(z) = z^2/2$ , is the locus of all points with a smaller  $n$ -ratio and full overlap. Next consider the changes in these regions when  $z$  is increased by a differential  $dz$ . Note that sides AC and AD sweep two triangles of combined area  $dA_1 = dz$ , and side CD sweeps a rectangle of area  $dA_2 = zdz$ . The expected overlap is the weighted mean of the average overlap for the pedestrians found in each of these two differential regions: the two swept triangles and the swept rectangle. In the two triangles the average overlap is  $2/3$  (ranging from 0 at vertex A to 1 at the opposite bases) and in the rectangular region, 1. This leads to (4a), below. Furthermore, since the “ $n$ -ratio” is  $z/2$  in our differential regions, every pedestrian there satisfies:  $L = (z/2)O$ , so we can write,  $E(L|z) = (z/2)E(O|z)$  and obtain (4b). Thus, we have:

$$E(O|z) = \frac{2/3 dA_1 + dA_2}{dA_1 + dA_2} = \frac{2/3 dz + zdz}{dz + zdz} = \frac{2 + 3z}{3 + 3z}, \quad (4a)$$

and

$$E(L|z) = (z/2)E(O|z) = \frac{2z + 3z^2}{6 + 6z}. \quad (4b)$$

The unconditional expectations are now obtained by averaging (4) over the distribution of  $z$ . The cumulative distribution function of  $z$  is given by:

$$F_z(x) = \Pr\{z \leq x\} = 1 - \exp(-f(A_1(x) + A_2(x))) = 1 - \exp(-f(x + 1/2x^2)). \quad (5)$$

It follows that:

$$E(O) = \int_0^\infty \frac{2 + 3x}{3 + 3x} dF_z(x) = \int_0^\infty (2/3 + x) f \exp(-f(x + 1/2x^2)) dx, \quad (6a)$$

and

$$E(L) = \int_0^\infty \frac{2x + 3x^2}{6 + 6x} dF_z(x) = \int_0^\infty (x/3 + x^2/2) f \exp(-f(x + 1/2x^2)) dz. \quad (6b)$$

Thus, the expression for the proposed upper bound is:

$$q_o^U = \frac{E(L)}{E(L) + E(O)}, \quad (7)$$

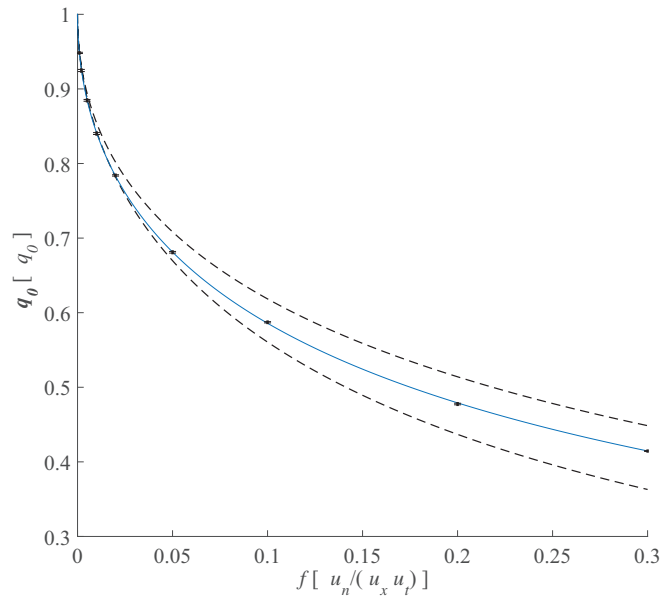


Fig. 3. Capacity as function of the pedestrian flux. Symbols in brackets are measurement units.

where  $E(L)$  and  $E(O)$  are given by (6). Because the integrals in (6) are Gaussian, they can be expressed after some manipulation in terms of the pdf,  $\phi$ , and complementary cdf  $\tilde{\Phi}$ , of the standard normal random variable evaluated at  $\sqrt{f}$ . The final result is:

$$q_o^U = \frac{\tilde{\Phi} \cdot (3 + f) - \phi \cdot \sqrt{f}}{\tilde{\Phi} \cdot (3 - f) + \phi \cdot 5\sqrt{f}}. \quad (8)$$

The top curve of Fig. 3 graphs this expression.

For small and large values of  $f$  the above can be seen to satisfy:

$$1/q_o^U = 1 + \sqrt{8f/\pi} + o(\sqrt{f}), \quad \text{as } f \rightarrow 0, \quad (9a)$$

and

$$1/q_o^U = 2f + o(f), \quad \text{as } f \rightarrow \infty. \quad (9b)$$

The next section derives a lower bound that turns out to have similar asymptotics. This similarity implies that the function  $q_o(f)$  must share these asymptotic features. This knowledge is exploited in Section 3.3 to develop a simple approximation for  $q_o(f)$ .

### 3.2. A lower bound

Recall that: the cost associated with a feasible path is the fraction of time that it does not overlap with bottlenecks,  $\sum L_i / (\sum O_i + \sum L_i)$ ; that the conditional capacity is the smallest  $\sum L_i / (\sum O_i + \sum L_i)$  across all feasible paths; and that  $q_o$  is the average of these minima across realizations.

Clearly then,  $q_o$  is bounded from below by any quantity that bounds from below every realized instance of  $\sum L_i / (\sum O_i + \sum L_i)$ . One such bounding quantity, denoted  $q_o^L$ , is constructed below by replacing every  $O_i$  in this expression by an upper bound and every  $L_i$  by a lower bound.

Since  $O_i \leq 1$ , the upper bound chosen for  $O_i$  is 1. And, since  $L_i$  is the duration of a valid non-overlapping segment to another bottleneck, the lower bound chosen for  $L_i$  is the duration,  $M_i$ , of a valid segment that reaches another bottleneck in the least time possible. Thus, our lower bound is  $q_o^L \equiv \sum M_i / (\sum 1 + \sum M_i) = \bar{M} / (\bar{M} + 1)$ ; or  $1/q_o^L = 1 + 1/\bar{M}$ , where the overlines denote the arithmetic means.

A formula for  $\bar{M}$  is now derived. Since our pedestrian arrival process is time- and space-independent, and ergodic,  $\bar{M}$  can be evaluated assuming that the segment's starting point is at the origin. Thus,  $\bar{M}$  is the expected duration  $E(M)$  of a valid segment from the origin that reaches a bottleneck in the least time possible.

The calculation uses the logic of Section 3.1. Note from the geometry of Fig. 2 that the least duration satisfies  $M > z/2$  if and only if the closed pentagon ABCDE of the figure does not contain any pedestrians. Since the area of ABCDE is  $2z + z^2/2$ , we can write:

$$\Pr\{M > z\} = \exp(-f[4z + 2z^2]), \quad (10)$$



and

$$\bar{M} \equiv E(M) = \int_0^\infty \exp(-f[4z + 2z^2])dz. \quad (11)$$

Now reorganize the exponent of (11) to read  $-f[4z + 2z^2] = -1/2[4f(z+1)^2 - 4f]$  and introduce the change of variable,  $4f(z+1)^2 \equiv y^2$  to find:

$$\bar{M} = \frac{\exp(2f)}{\sqrt{4f}} \int_{\sqrt{4f}}^\infty \exp(-1/2y^2)dy = \left[2\pi \frac{e^{4f}}{4f}\right]^{1/2} \tilde{\Phi}(\sqrt{4f}). \quad (12)$$

Therefore:

$$1/q_o^L = 1 + \left[\frac{2f}{\pi e^{4f}}\right]^{1/2} \left[\tilde{\Phi}(2\sqrt{f})\right]^{-1}. \quad (13)$$

This expression is depicted by the bottom curve in Fig. 3. The reader can verify that the asymptotics of (13) are:

$$1/q_o^L = 1 + \sqrt{8f/\pi} + o(\sqrt{f}), \quad \text{as } f \rightarrow 0, \quad (14a)$$

and

$$1/q_o^L = 4f + o(f), \quad \text{as } f \rightarrow \infty. \quad (14b)$$

### 3.3. An approximation

Simulations with Newell's car-following model (Newell, 2002) which are described in the Appendix were compared with the bounds, and then used to calibrate an approximate formula. These comparisons helped us identify and correct flaws in the simulation's original assumptions that detracted from realism. The bounds also inspired the functional form of the calibrated capacity formula.

Regarding assumptions, it was found that the spatial indivisibility of cars in the simulation affected the results significantly for high pedestrian fluxes. As a result it was necessary to ensure that the simulation included a realistic mechanism for pedestrians and cars to resolve spatial conflicts. To illustrate the necessity of this feature consider two pedestrians that cross simultaneously at two locations less than one jam spacing apart. The KWT/VT model on which our bounds are based will allow part of a car to be stored in between the pedestrians, and to be released as soon as the downstream pedestrian has crossed. But in reality (and in a properly implemented car-following model) no cars would fit and no flow could be released. Thus, the KWT/VT flow predictions are optimistic when the pedestrian flux is so high that nearby pedestrian crossings occur often. Furthermore, spatial indivisibility also implies that pedestrians must adapt their crossing paths when they step across a line of stopped cars, so they are restricted to move in channels between cars. This channelization, which was included in the car-following model, concentrates pedestrian movements onto virtual crosswalks and therefore also acts to depress car flow. Our simulations showed that spatial indivisibility reduces capacity by an increasing percentage as  $f$  increases. For low values the reduction is insignificant (about 0.2% for  $f = 0.002$ ) but for  $f = 0.3$  the reduction was 5%.

Regarding the structural form of the capacity formula, consider the following. A comparison of (9) and (14) reveals that the asymptotics for these bounds match for low  $f$  and are of the same order for high  $f$ . Since the KWT/VT version of  $q_o$  must lie in between these bounds, the KWT/VT capacity function must have the same asymptotics for low  $f$  and be of the same order for high  $f$ . In other words, the KWT/VT capacity must satisfy the following for some constant  $a \in [2, 4]$ :

$$1/q_o = [1 + \sqrt{8f/\pi}] + o(\sqrt{f}), \quad \text{as } f \rightarrow 0, \quad (15a)$$

and

$$1/q_o = [af] + o(f), \quad \text{as } f \rightarrow \infty. \quad (15b)$$

Note, since the bracketed term on the RHS of (15a) is  $o(f)$  as  $f \rightarrow \infty$ , it could be substituted for the second term in (15b). Likewise, the bracketed term on the RHS of (15b) is  $o(\sqrt{f})$  as  $f \rightarrow 0$ , so it could be substituted for the last term of (15a). It follows that the sum of these bracketed terms, plus a third term of the form  $b f^c$  where  $c \in (0.5, 1)$ , would satisfy both equations. Thus, a simple functional form for the KWT/VT capacity with the correct asymptotics is  $1/q_o \approx 1 + \sqrt{8f/\pi} + af + b f^c$ , with  $a \in [2, 4]$  and  $c \in (1/2, 1)$ . However, because the real capacity is lower than the KWT capacity for large  $f$ , the condition  $a \in [2, 4]$  stemming from (15b) for  $f \rightarrow \infty$  should be relaxed and replaced by  $a \geq 0$  for the real capacity.

With this in mind, the parameters  $a, b, c$  were chosen by fitting the expression  $1/q_o \approx 1 + \sqrt{8f/\pi} + af + b f^c$  to the simulated capacities. Fig. 3 shows the simulated capacities by means of dots, with vertical lines denoting the simulation error. The lines are nearly invisible because the simulations were run for a very long time to make the statistical error insignificant; see Appendix for more detail. It was found that the choice  $a = 1.27, b = 0.35, c = 2/3$  kept all the discrepancies to well under 0.2%; i.e. to less than a handful of cars in one hour of observation for a single lane. The adopted expression,

$$q_o(f) \approx 1/(1 + \sqrt{8f/\pi} + 1.27f + 0.35f^{2/3}), \quad \text{for } f \in [0, 0.3], \quad (16)$$

is depicted by the middle curve of Fig. 3. Note the good fit.

#### 4. The macroscopic fundamental diagram

This section establishes that the MFD stemming from KWT/VT is concave and symmetric with respect to the line  $k = 1/2$ . Hence  $k_0 = 1/2$ . It then derives an exact expression for the free-flow speed of the pedestrianized street. Finally, based on these two facts and on the capacity expression (16), an approximate expression for the real MFD is proposed. This expression is derived in dual coordinates and then re-expressed in primal coordinates in an arbitrary system of units for ease of application. The result is compared with simulations.

**Concavity:** The conditional MFD for any pedestrian realization is the lower envelope of the family of “cuts”  $\{q = c(u) + uk; \forall u \in [-2, 2]\}$ , where  $c(u)$  is the least cost of an infinitely long valid path with average slope  $u$ . As such, the conditional MFD is everywhere below its tangents, so it is concave. And since the MFD,  $Q(k)$ , is the average of these concave functions, it is itself concave.

**Symmetry:** This is established with a model of empty spaces or “holes”. We imagine that at all times the street is uniformly filled to jam density with a combination of vehicles and “holes” and focus on the movement of holes. Since the sum of holes and vehicles is fixed, when a vehicle advances past an observer, a hole must flow in the opposite direction; i.e., the two flows cancel out. Furthermore, the sum of the densities of holes and vehicles must be 1. So, if we use tildes to denote the flow, speed and density variables associated with holes, we have that:  $k + \tilde{k} = 1$  and  $q = -\tilde{q}$  at every time and location. Therefore, in a steady state with densities  $k$  and  $\tilde{k} = 1 - k$  it must be true that  $Q(k) = -\tilde{Q}(\tilde{k})$ ; i.e., holes obey the same FD as cars except for a sign reversal. Consideration also shows that if the flow of cars is interrupted by a bottleneck, so is the flow of holes. Thus, except for the sign reversal that corresponds to the change in direction, holes obey the same dynamic model as cars. Therefore we can write,  $Q(k) = -\tilde{Q}(\tilde{k})$ . In addition,  $\tilde{Q}(\tilde{k}) = -Q(1 - k)$  because the flows of holes and cars must cancel out. The last two equalities show that  $Q(k) = Q(1 - k)$ ; i.e., that the MFD is symmetric with respect to the line  $k = 1/2$ . Hence  $k_0 = 1/2$ .

**Free flow speed:** To estimate  $v_f$  consider the expected time required by an isolated car to travel a distance  $\Delta x \rightarrow 0$ . This time is  $\Delta x/v_f = \Delta x/2$  if the car is not interrupted by a pedestrian. An interruption happens if a pedestrian arrives in the window of space-time preceding the car by a time duration  $\tau = 1$ , and the average duration of any such interruption is  $1/2$  time units. Since the pedestrian flux is  $f$  and the window size is  $\Delta x \rightarrow 0$ , an interruption occurs with probability  $f\Delta x$ . For  $\Delta x \rightarrow 0$  the probability of multiple interruptions is  $O(\Delta x^2)$ . Thus, since  $\Delta x \rightarrow 0$ , the expected delay added by interruptions is  $f\Delta x/2$ . Hence, interruptions add  $f/2$  units to the vehicle's pace so that the free-flow pace is:

$$1/v_f = 1/v_f + f/2 = (1 + f)/2. \quad (17)$$

**MFD approximation:** A first order approximation for the MFD for low values of  $k$  is  $Q(k) \approx v_f k$ . A second order approximation that should work well for values close to the optimum density ( $k = 1/2$ ) is  $Q(k) \approx v_f k + P(k)$ , where  $P(k)$  should be non-positive, concave, satisfy  $P = 0$  and  $dP/dk = 0$  for  $k = 0$ , and also satisfy  $P = q_0 - v_f/2$  and  $dP/dk = -v_f$  for  $k = 1/2$ . A simple function with the first four of these properties is the power of  $k$ ,  $P(k) = \alpha k^\beta$  with  $\alpha < 0$  and  $\beta > 1$ . The values of  $\alpha$  and  $\beta$  are then chosen so that the last two properties (for  $k = 1/2$ ) are satisfied. The result of these manipulations yields a formula for  $Q(k)$  that should work well for  $k \in [0, 1/2]$ . For  $k \in (1/2, 1]$  the symmetry relation  $Q(k) = Q(1 - k)$  can be used. The end result is:

$$Q(k) = Q(1 - k) \approx q_0 [\gamma(2k) + (1 - \gamma)(2k)^{\gamma/(\gamma-1)}], \quad \text{where } \gamma = \frac{v_f}{2q_0} \text{ and } k \in [0, 1/2]. \quad (18)$$

In the above,  $q_0$  is given by (16) and  $v_f$  by (17).

**MFD formulas in ordinary coordinates and natural units:** For ease of application, Eqs. (16)–(18) are now re-expressed in synchronous time using variables and parameters endowed with dimensions in a consistent system of units; i.e., as one would naturally use in formulating the problem in an ordinary coordinate system. These natural variables and parameters will be denoted by double primes. Variables and parameters without primes (e.g.,  $v$ ,  $k$ ,  $q$ ) continue to be the dimensionless dual variables we have been using so far; and variables with single primes will be dimensionless primal variables.

To start let us transform the dual versions of pace, density and speed into natural units. For pace this is done in two steps: (i) transform the dual dimensionless pace into primal dimensionless form; and (ii) endow the result with dimensions using the natural unit of pace,  $k_j''/q_0''$ . Step (i) is expressed by Eq. (2). Recall, however, that in this expression, primes had not yet been dropped for dual variables. Rewritten in our current notation Eq. (2) is:  $1/v = 1/v' - 1/u'$ , where  $1/u' = k_0' - \frac{1}{2}$ . Step (i) is completed after rearranging terms and writing:  $1/v' = 1/v + k_0' - \frac{1}{2}$ . Step (ii) is performed by multiplying both sides of this equality by  $k_j''/q_0''$ . The left hand side simplifies to  $1/v'(k_j''/q_0'') \equiv 1/v''$  since  $(k_j''/q_0'')$  is the natural unit of pace. The right hand side becomes  $1/v(k_j''/q_0'') + k_0'(k_j''/q_0'') - \frac{1}{2}(k_j''/q_0'')$ ; and since the natural unit of density is  $k_j''$ , the numerator of the second term simplifies to:  $k_0'k_j'' = k_0''$ . The final result is Eq. (19a) below. Equations (19b) and (19c) are easily obtained using the identity  $q'' \equiv qq_0''$ , which holds because the primal-dual transformation leaves flow invariant and the natural unit of flow is  $q_0''$ . Equation (19b) is the product of the identity and (19a); and Eq. (19c) is the special case of the identity for MFD flows.

$$1/v'' = 1/v(k_j''/q_0'') + (k_0'' - k_j''/2)/q_0'': \quad (19a)$$

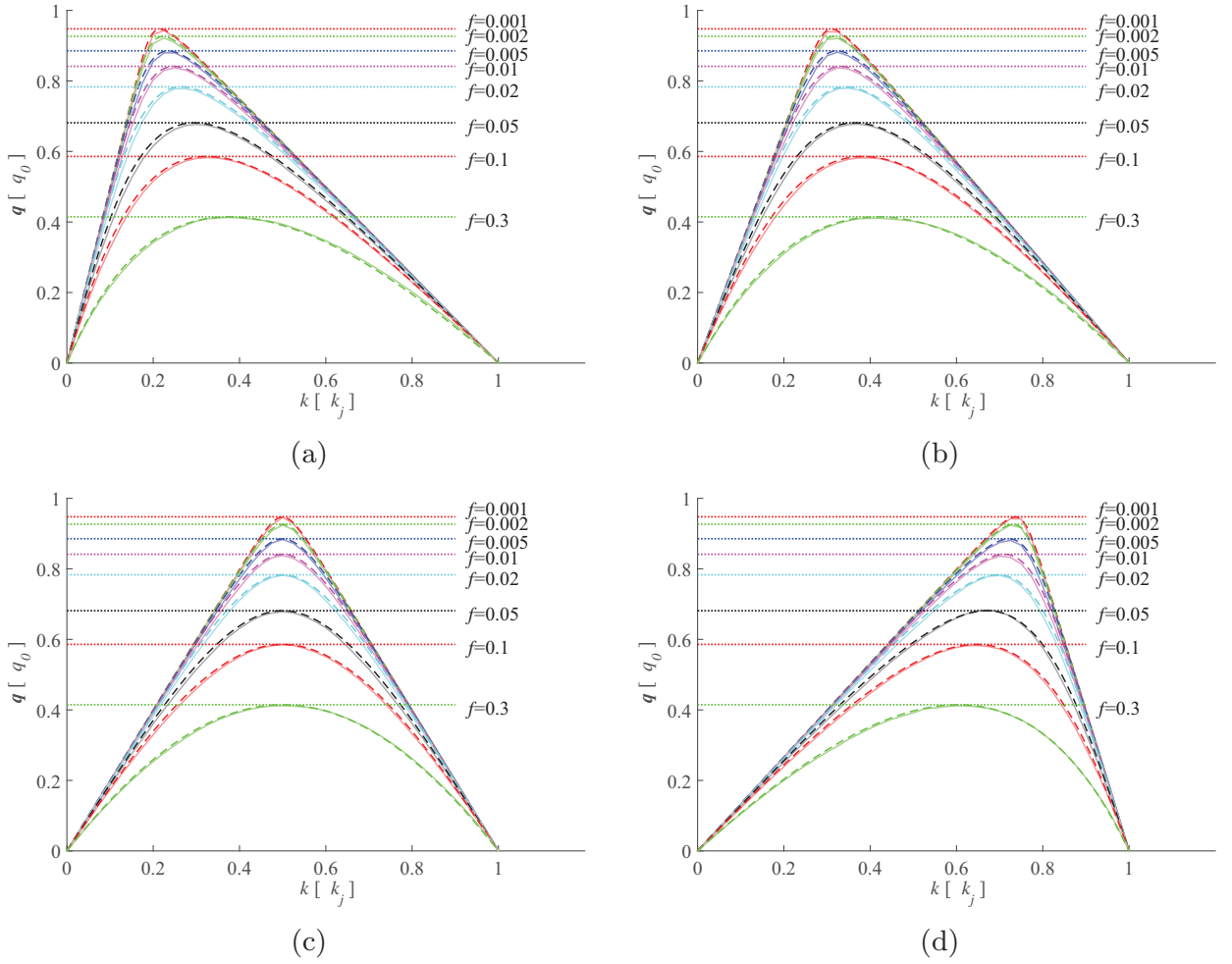


**Fig. 4.** Estimated MFD's for four values of  $k_0$ . (a)  $k_0 = 0.2$ ; (b)  $k_0 = 0.3$ ; (c)  $k_0 = 0.5$ ; (d)  $k_0 = 0.75$ . Symbols in brackets are the measurement units. Solid lines are simulated results and dotted lines analytical estimates. The horizontal lines indicate the values of the estimated capacity.

$$k'' = k k_j'' + q(k_o'' - k_j''/2); \quad (19b)$$

$$q'' = q_o'' q. \quad (19c)$$

Since both the car flow and the pedestrian flux are invariant, the only change in (16) is the rescaling implied by (19c) and the re-expression of the dimensionless pedestrian flux by  $f''\tau''/k_j''$ . Thus, the capacity formula becomes:

$$q_o'' \approx q_o'' / \left( \sqrt{\frac{8f''\tau''}{\pi k_j''}} + 1.27 \frac{f''\tau''}{k_j''} + 0.35 \left( \frac{f''\tau''}{k_j''} \right)^{2/3} \right). \quad (20)$$

The free-flow speed transforms as per (19a):

$$1/v_f'' = 1/v_f(k_j''/q_o'') + (k_o'' - k_j''/2)/q_o'', \quad (21)$$

where  $v_f$  is given by (17).

To transform the MFD consider that (19b) and (19c) associate with each point of the dual MFD  $\{k, Q(k)\}$  the primal point:

$$k''(k) = k k_j'' + Q(k)(k_o'' - k_j''/2); \quad (22a)$$

$$q''(k) = q_o'' Q(k). \quad (22b)$$

As  $k$  is varied in  $[0, 1]$ , these two equations describe the arbitrary-unit, primal MFD curve.

The primal optimum density is now obtained by setting  $k = 1/2$  and  $\mathbf{Q}(1/2) = \mathbf{q}_0$  in (22a). The result is:

$$\mathbf{k}_0'' \approx 1/2 \mathbf{k}_j'' + \mathbf{q}_0(\mathbf{k}_0'' - \mathbf{k}_j''/2), \quad (23)$$

where  $\mathbf{q}_0$  is given by (16)

**Comparison with simulations:** Fig. 4 compares the MFD predicted by (22) with simulations involving discrete vehicles; solid lines are the analytic results and dashed lines the simulations. The figure reveals that the fit is good enough for use in practical applications for all values of the parameters, especially along the uncongested branch which is the one likely to arise in practice.

## 5. Discussion

The formulas of this paper should also apply approximately if the pedestrian crossing times are mutually independent random variables with mean  $\tau$  and a finite standard deviation. This is conjectured because the derivations of the free-flow speed and the capacity's lower bound can be repeated with random crossing times, and their results are the same as in the deterministic case. Furthermore, although the proposed upper bound could change a little when randomness is introduced, simpler upper bounds that have the same asymptotic behavior as the proposed bound for low  $f$  do not change.<sup>4</sup> Thus, the proposed capacity formula should work similarly well for low  $f$ 's with random crossing times.

In principle, the MFD formula could be improved by obtaining approximations for all the “cuts” corresponding to all valid observer speeds, and estimating the MFD by the lower envelope of all the cuts. Unfortunately, we have found that the formula for the cut with average observer speed zero (which yields the capacity) is easier to obtain than the rest. Thus, the cut-approach seems unpromising for the pedestrian problem. The cut-approach has been tried for a related problem involving signalized arterials (see, e.g., Daganzo and Geroliminis, 2008, and Laval and Castrillon, 2015) but the observers used to obtain the cuts in these works are not allowed to reverse directions, unlike those used for the pedestrianized street. For this reason the approximations proposed in these papers are not always accurate and improved methods based on sufficient networks, similar in spirit to the approach in this paper, have been proposed (Leclercq and Geroliminis, 2013). Further explorations should improve the accuracy these methods, in particular for inhomogeneous streets, hopefully yielding exact recipes for the MFD.

Finally, the results in this paper pertain to homogeneous pedestrian fluxes. We expect this to be a best case scenario since inhomogeneous flux distributions should lead to higher delays for isolated cars and less throughput flow. Thus, research to explore the effects on inhomogeneous distributions is desirable. We anticipate that this type of research can benefit, both, from the dimensional simplifications introduced in Section 2 and from VT.

## Acknowledgment

Research supported by research grant 65A0529 from UC-Connect and a research grant from the Netherlands Organisation of Scientific Research. The comments of the reviewers are gratefully acknowledged.

## Appendix. Simulations for model calibration and verification

A simulation program was used to calibrate the capacity formula and to verify that the MFD formulae were reasonable. Cars were assumed to be  $k_j$  distance units long, be indivisible and follow Newell (2002) car-following model. Pedestrians were treated as point bottlenecks that arose at random locations in space-time and lasted  $\tau$  time units. For maximum realism, pedestrians generated next to a line of stopped cars were required to cross in between the cars. It was assumed that pedestrians would cross where their lateral displacement would be smallest, so this displacement is at most  $k_j/2$ . Fig. A.5a shows an example set of trajectories for one of the simulation runs.

The simulation was implemented for a circular street as this allowed us to use a fixed number of vehicles and control for density. The simulations were run using real-world units:  $q_0 = 1800$  veh/h,  $v_f = 9$  m/s and changing  $k_j$ . A 0.1 s simulation time step was used to ensure that it was small compared with the pedestrian crossing times, which were fixed at  $\tau = 10$ s. Each simulation run was started with a warm up period in which the vehicles were generated at uniformly distributed locations at a speed matching the speed derived from the fundamental diagram for that density. Pedestrians were introduced from time  $1/r$  in order to be able to create the Newell trajectories. The crossing locations of the pedestrians arriving in each time step were displaced as explained above when necessary. As the simulation ran, Edie's generalized flow in each time window of 60 s was evaluated (Edie, 1963). Recall this is the ratio of the total distance traveled by all cars in the window, and the product of the time-window duration and the street length.

In all cases simulated the system transitioned into equilibrium in well under  $10^3$  simulation steps, which correspond to well under 10 pedestrian crossing times – around 10 min. Fig. A.5b shows these initial effects for one of the simulated

<sup>4</sup> An example is a bound based on a myopic algorithm like the one used in this paper that instead of selecting the pedestrian whose bottleneck can be reached with the smallest n-ratio, selects the pedestrian bottleneck that can be reached in the least time.

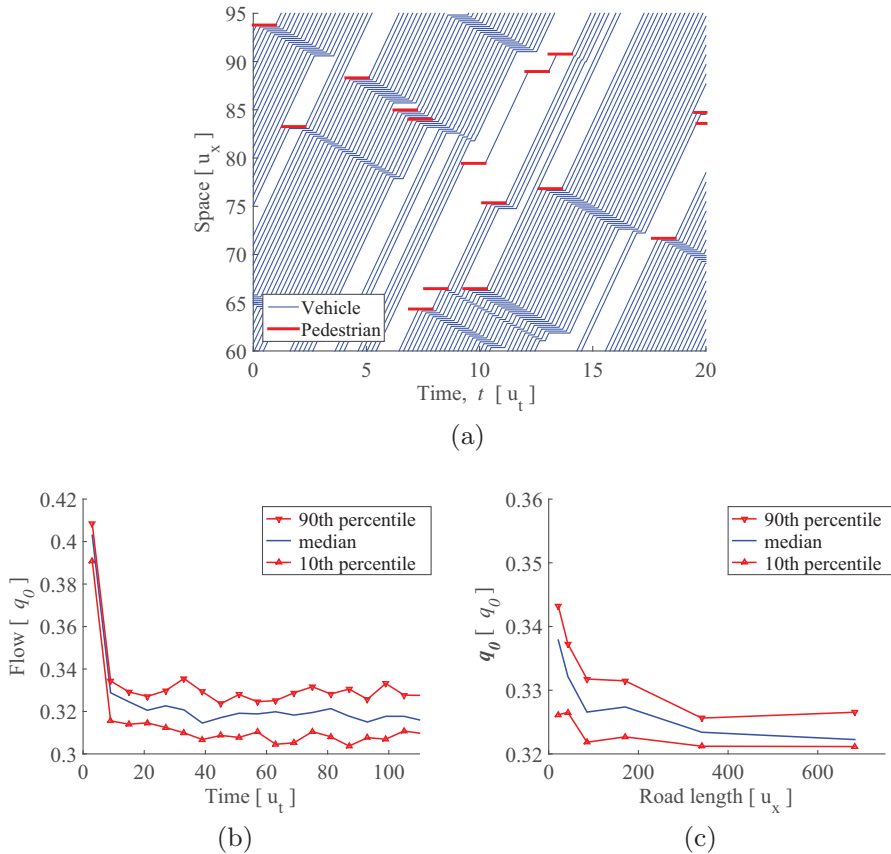


**Fig. A1.** Car-following model features [symbols in brackets are measurement units]: (a) A set of simulated vehicle trajectories for a pedestrian realization; (b) time-series of the street's flow showing the initial transient; (c) the effect of street length on flow.

scenarios. By doubling the street length multiple times (see Fig. A.5c) a length was found for which the results did not change after further doublings; i.e., a length that emulated an infinite street. Based on this analysis, we chose  $L = 15,460$  m.

Nine different scenarios with different values of the dimensionless pedestrian flux were simulated:  $f = \{0.001; 0.002; 0.005; 0.01; 0.02; 0.05; 0.1; 0.2; 0.3\}$ . For each of these scenarios, the average system flow was evaluated for 40 different densities uniformly distributed in the range  $(0, k_j) \equiv (0, 1)$ ; and the highest resulting flow was selected as the estimate of  $q_0$ . For each density, the simulation was run for 750 min. The results for the first 100 min were discarded to eliminate any initial transient. To have an idea of the estimation error, the retained part of the simulations were broken into consecutive mini-run windows of 50 min each. The mean flows in these windows were then treated as a sample of (average) flow observations because the standard error of this sample's mean is an estimator for the error in our estimate. These (very small) errors are shown on Fig. 3 by means of vertical bars.

## References

- Daganzo, C.F., 1977. Traffic delay at unsignalized intersections: Clarification of some issues. *Transportation Science* 11, 180–189.
- Daganzo, C.F., 1997. *Fundamentals of Transportation and Traffic Operations*. Pergamon-Elsevier, New York, N.Y.
- Daganzo, C.F., 2002. *A Theory of Supply Chains*, 526. *Lecture Notes in Economics and Mathematical Systems*. Springer, Berlin, Germany.
- Daganzo, C.F., 2005a. A variational formulation of kinematic waves: basic theory and complex boundary conditions. *Transportation Research Part B* 39 (2), 187–196.
- Daganzo, C.F., 2005b. A variational formulation of kinematic waves: solution methods. *Transportation Research Part B* 39 (10), 934–950.
- Daganzo, C.F., 2006. On the variational theory of traffic flow: well-posedness, duality and applications. *Networks and Heterogeneous Media* 1 (4), 601–619.
- Daganzo, C.F., Geroliminis, N., 2008. An analytical approximation for the macroscopic fundamental diagram of urban traffic. *Transportation Research Part B* 42 (9), 771–781.
- Edie, L.C., 1963. Discussion of traffic stream measurements and definitions. *Proceedings of the 2nd International Symposium on the Theory of Traffic Flow*. OECD, Paris, France, pp. 139–154.
- Feller, W., 1968. *An Introduction to Probability Theory and its Applications*, Vol I, third ed. John Wiley and Sons, New York, N.Y.
- Hawkes, A.G., 1965. Queuing for gaps in traffic. *Biometrika* 52, 79–85.
- Hawkes, A.G., 1968. Gap acceptance in road traffic. *Journal of Applied Probability* 5, 84–92.
- Laval, J.A., Castrillon, J., 2015. Stochastic approximations for the macroscopic fundamental diagram of urban networks. *Transportation Research Part B* 81, 904–916.
- Leclercq, L., Geroliminis, N., 2013. Estimating MFDs in simple networks with route choice. *Transportation Research Part B* 57, 468–484.

- Lighthill, M.J., Whitham, G.B., 1955. On kinematic waves. i flow movement in long rivers. II A theory of traffic flow on long crowded roads. *Proceedings of the Royal Society A* 229, 281–345.
- Newell, G.F., 1979. Approximate Behavior of Tandem Queues, 171. *Lecture Notes in Economics and Mathematical Sciences*. Springer-Verlag, Berlin, Germany.
- Newell, G.F., 1993. A simplified theory of kinematic waves: (i) general theory; (ii) queuing at freeway bottlenecks; (iii) multi-destination flows. *Transportation Research Part B* 37, 281–313.
- Newell, G.F., 2002. A simplified car-following theory: a lower order model. *Transportation Research Part B: methodological* 36, 195–205.
- Richards, P.I., 1956. Shockwaves on the highway. *Operations Research* 4, 42–51.
- Tanner, J.C., 1951. The delay to pedestrians crossing a road. *Biometrika* 39, 383–392.